Supplemental material to the article

Pade spectroscopy of structural correlation functions: application to liquid gallium

1 Peak detection in the radial distribution function.

In statistical mechanics, the radial distribution function (or pair correlation function) $g(r)$ of a system of particles (atoms, molecules, colloids, etc.) describes how density varies as a function of distance from a reference particle. The first peak of the radial distribution function describes particles in the first coordination sphere – "the nearest neighbours" of the given particle. In the Lennard-Jones fluid, the first peak of $g(r)$ is a smooth bell- shaped curve without apparent characteristic scales except the position of the peak maximum. In gallium, the first peak of $g(r)$ is not a smooth curve: there are features (shoulders, asymmetry) at distances shorter and longer than the position of the maximum.

The conventional method to distinguish such features is to perform peak analysis by some special program. It implies fitting of $g(r)$ by a series of peaks. As the result, the first peak of $g(r)$ is represented as superposition of subpeaks which can be interpreted as the distributions of particles forming particular local order. Then the sub-peak maxima locations should be treated as the most probable distances between particles forming the local order clusters. The width of the sub-peaks show the accuracy of this interpretation. The nearest subpeaks obviously should not overlap too much.

The result of the peak analysis is shown in Fig. 1. We have used the standard program that fits experimental data by a superposition of separate peaks, each of which can be described by one of the standard functions given below (for the complete list of peak-functions see the web-site of the program manufacture). We see that the results strongly depend on the kind of the peak function we choose for analysis! The final result is quite accurate for all the cases but the position of the peaks, their width and height strongly depend on the peak basis we have chosen. So the standard peak analysis does not reliably work for $g(r)$ because features of the function are not so pronounced.

Pade-approximation and analytical continuation into the complex plain of r is in fact an advanced peak analysis tool. It is capable of distinguishing peaks when features of $g(r)$ are not very pronounced. Pade-spectroscopy allows to determine with high accuracy the exact position of the peak (real part of the pole in complex plane) corresponding to the features in $g(r)$ and its width (imaginary part of the pole in complex plane).

By the way, peak analysis shown in Fig. 1a is quite accurate. We applied the Pade-based analytical continuation method to approximant produced by the peak-analysis program, Fig. 1a. We have got the picture of poles close to that obtained by the direct analysis of $g(r)$-table using Pade (Fig. 1 in the paper): real parts of the pole positions are well reproduced but the imaginary parts (width of the peaks) corresponded not so well. This test confirms the validity of "Pade-spectroscopy" method as the reliable tool for determination with high accuracy the peaks corresponding to the features in $g(r)$. We should repeat again that Pade analysis of the peaks is free from ambiguity of the standard peak-analysis program related to the choice of the peak-basis and the corresponding approximation errors.

Pade peak analysis method is applicable not only for $g(r)$ but for any function with features.

Basic peak shape formulas available in NETZSCH Peak Separation program:

General shape: The general shape of peak is the weighted mixture of Fraser–Suzuki and asymmetric Cauchy.

$$y(x) = \mathrm{Ampl}\left[\mathrm{Part}\,\exp(-\mathrm{Coef}^2 \ln 2) + \frac{1-\mathrm{Part}}{1+\mathrm{Coef}^2}\right], \tag{1}$$

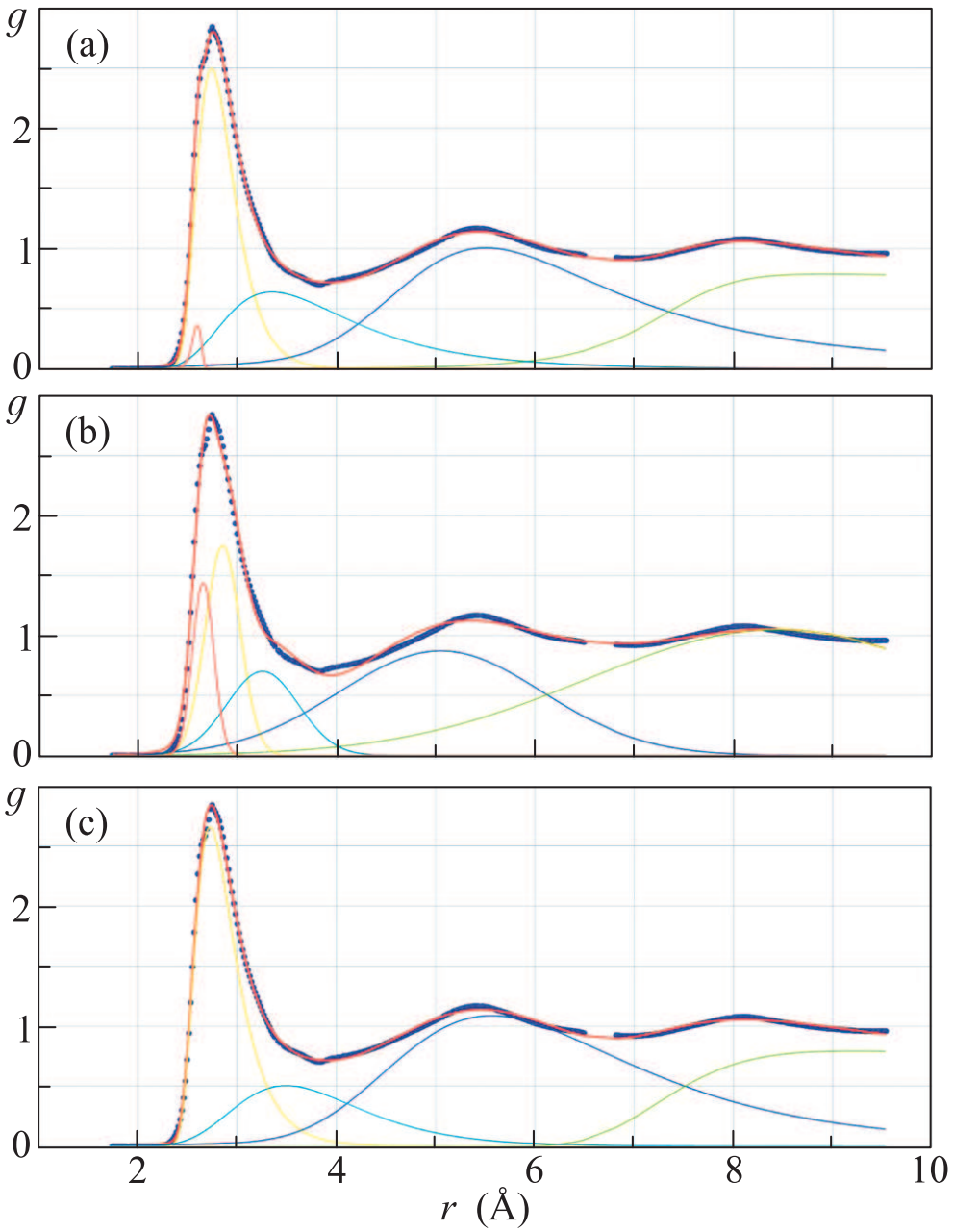

Figure 1: Experimental radial distribution function $g(r)$ of liquid gallium for $T = 313$ K approximated by different functions. (a) – General peak approximants. (b) – Gaussian approximants, and c) Cauchy approximants

where

$$\text{Coef} = \frac{\ln[1 + 2\text{Asym}(x - \text{Pas})/\text{Hvd}]}{\text{Asym}}. \tag{2}$$

Here Part, Asym, Pas, Hvd are the fitting parameters.

Pseudo-Voit: If Asym=0, then peak shape is the Pseudo-Voit shape (weighted mixture of Gauss and Cauchy).

$$y(x) = \mathrm{Ampl}\left[\mathrm{Part}\,\exp(-\mathrm{Coef}^2\ln 2) + \frac{1-\mathrm{Part}}{1+\mathrm{Coef}^2}\right], \tag{3}$$

where

$$\mathrm{Coef} = 2(x-\mathrm{Pas})/\mathrm{Hvd}. \tag{4}$$

Cauchy: If $\mathrm{Part} = 0$ **and** $\mathrm{Asym} = 0$ **then peak shape is Cauchy shape.**

$$y(x) = \mathrm{Ampl}\frac{1-\mathrm{Part}}{1+(2[x-\mathrm{Pas})/\mathrm{Hvd}]^2}. \tag{5}$$

Gauss: If $\mathrm{Part} = 1$ **and** $\mathrm{Asym} = 0$ **then peak shape is Gauss shape.**

$$y(x) = \mathrm{Ampl}\,\mathrm{Part}\exp\left\{-[2(x-\mathrm{Pas})/\mathrm{Hvd}]^2\,\ln 2\right\}. \tag{6}$$

2 Pade approximants method.

Here we discuss the construction of the Padé approximants that interpolate a function given N knot points. Pade-approximants are the rational functions (ratio of two polinomials). A rational function can be represented by a continued fraction. Typically the continued fraction expansion for a given function approximates the function better than its series expansion. Here we use "multipoint" algorithm [1–3] to build the Pade-approximant. Suppose we know function values $f(x_i) = u_i$ in the discrete set of points x_i where the "knots" x_i, $i = 1, 2, 3, \ldots, N$. Then the Pade approximant

$$C_N(x) = \cfrac{a_1}{\cfrac{a_2(x-x_1)}{\cfrac{a_3(x-x_2)}{\cfrac{a_4(x-x_3)}{\ldots a_N(x-x_{N-1})+1}+1}+1}+1}, \tag{7}$$

where a_i we determine using the condition, $C_N(x_i) = u_i$, which is fulfilled if a_i satisfy the recursion relation

$$a_i = g_i\left(x_i\right), \qquad g_1\left(x_i\right) = u_i, \qquad i = 1, 2, 3, \ldots, N, \tag{8}$$

$$g_p(x) = \frac{g_{p-1}(x_{p-1}) - g_{p-1}(x)}{(x-x_{p-1})\,g_{p-1}(x)}, \qquad p \geq 2. \tag{9}$$

Eq. (8) is the "boundary condition" for the recursive relation Eq. (9). For example, taking $x = x_{i_0}$ we get $g_1(x_i)$ from (8) and $g_j(x_{i_0})$, $j = 2, 3, \ldots, i$, from (9). Accuracy of the analytical continuation can be tested by permutations of x_i and/or by the random extraction of some part of the knots and permutation averaging.

There is important question related to the accuracy of numerical analytical continuation and stability of poles to errors in the initial data. We solve this problem doing two procedures.

We build the Pade-approximant on top known function values $f(x_i) = u_i$ in the discrete set of points x_i on the real axis. We always randomly shuffle the set of points x_i using the Fisher–Yates–Knuth shuffle algorithm [4] before building the Pade continued fraction approximant. Then we average the approximant over a considerable number of shuffles. This procedure helps avoiding specific errors related to numerical calculation of long continued-fraction.

Next, the accuracy of the Pade extrapolation of the function depends on the distribution of points x_i: maximum accuracy corresponds to the uniform distribution of x_i. Doing the stability test we randomly take away about 10 % of points x_i: this procedure makes the distribution of x_i nonuniform and moves the "unstable" poles in the complex plain if there are any. Finally we build the extrapolation $\tilde{f}$ of the function f averaging the Pade approximant over 10000 random extractions of initial points x_i. Then when we draw $|\tilde{f}(z)|$ at complex z, unstable poles disappear while the poles suffering from the insufficient accuracy of $f(x_i)$ average into "domes".

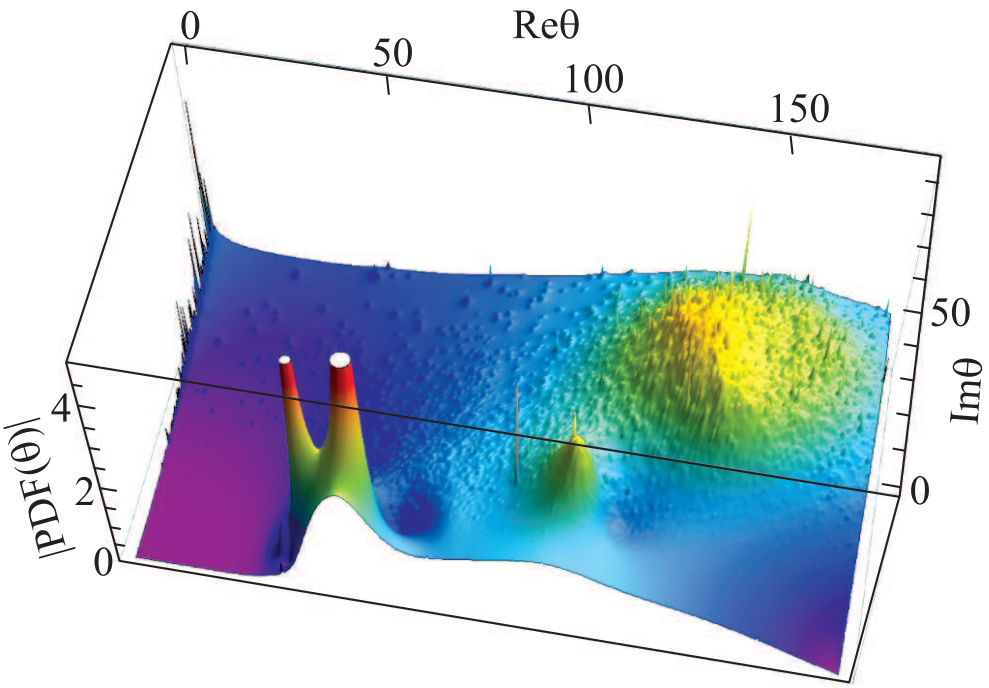

Figure 2: Stability test of PDF analytical continuation shown in Fig. 3b (see paper text)

This procedure is illustrated in Fig. 2. We test here PDF shown in Fig. 3b (see our paper) using the procedure described above. Poles at $\mathrm{Re}\,\theta \approx 44$ and ≈ 57 are stable. The other poles shown in Fig. 3b are not wrong, but their positions are more sensitive to the accuracy of the PDF-table. So after each random taking away some of the knots θ_i, the positions of the poles slightly change and finally after 10000 such procedures we see domes at the positions where in Fig. 3b we have seen poles. This test show that we can trust all the pole except, probably, one situated at $\mathrm{Re}\,\theta \approx 79$. (More refined stability test however shows that even this pole should not be completely disregarded.)

This procedure is illustrated in Fig. 2. We test here PDF shown in Fig.3b (see our paper) using the method described above. Poles at $\mathrm{Re}\,\theta \approx 44$ and ≈ 57 are stable. The other poles shown in Fig. 3b are not wrong, but their positions are more sensitive to the accuracy of the PDF-table. So after each random taking away some of the knots θ_i, the positions of the poles slightly change and finally after averaging over 10000 such extractions we see domes at the positions where in Fig. 3b we have seen poles. This test shows that we can trust all the poles except, probably, one situated at $\mathrm{Re}\,\theta \approx 79$. (More refined stability test however shows that even this pole should not be completely disregarded.) The coordinates of the "dome" top in the complex plain we should take then as the characteristic parameters. If we compare them with the coordinates of the poles in Fig. 3b we will see coincidence with the satisfactory accuracy.

3 Pade spectroscopy of LJ fluid.

For comparison, we investigated LJ fluid. We see two poles in the complex plain corresponding to the first peak of RDF (Fig. 3a). From the first glance the situation looks very strange, because it is not clear what characteristic scales one can find in LJ liquid except the first peak maximum position. Looking more attentively, one can see that, unlike liquid gallium, the poles in fact merge: the imaginary part of their position is larger then difference of the real parts. It is difficult to distinguish characteristic two scales in this situation. We can conclude, looking at Fig. 3, that there is one characteristic scale in RDF of LJ liquid around $r = 1$ that we can locate with the accuracy $\delta r \approx 0.15$. This

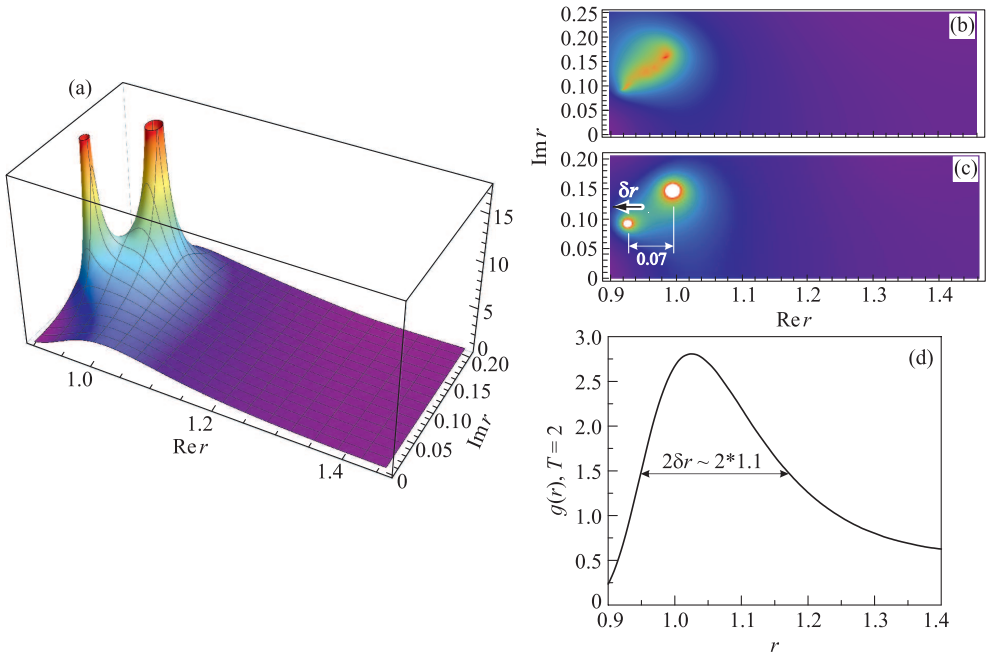

Figure 3: RDF of LJ liqud, $\rho = 1, T = 2$. (a) and (c) are analytical continuations: 3D and density plots of $|g(r)|$, (b) is the stability test of RDF analytical continuation when the the Pade approximant was averaged over 1 million random extractions of 20% of points from $g(r)$- table and (d) is $g(r)$.

conclusion also supports the stability test of RDF analytical continuation when the Pade approximant was averaged over 1 million random extractions of 20 % of points from $g(r)$-table, see Fig. 3b. Only the main peak at Re ≈ 1 is stable enough.

Similar Pade analysis we can do with PDF of LJ fluid, see Fig. 4. For density $\rho = 1$ the melting line is slightly below $T = 1.4$. We can distinguish three characteristic scales in PDF using analytical continuation: $\theta = 60, 110, 160$. These results agree with the common knowledge about the LJ fluid in this regime that its local order is mostly tetrahedral, see Ref. [5] and refs. therein for more details.

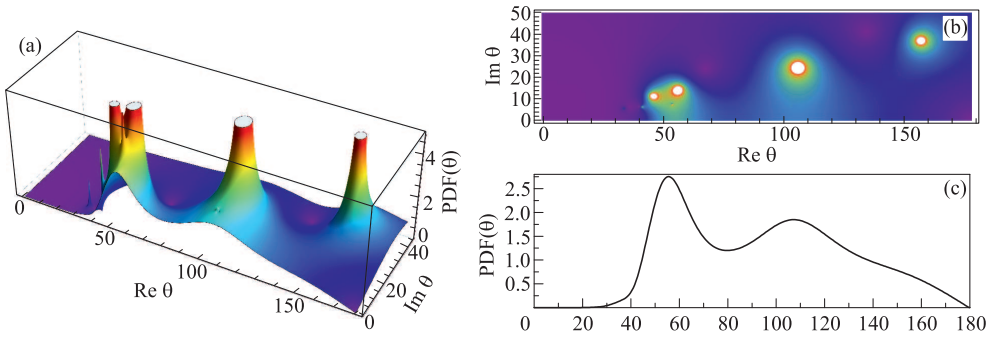

Figure 4: PDF of LJ liquid, $\rho = 1, T = 2$. (a, b) – Analytical continuations: 3D and density plots of $|\mathrm{PDF}(\theta)|$. (c) – $\mathrm{PDF}(\theta)$

References

[1] H. Vidberg and J. Serene, J. Low Temp. Phys. **29**, 179 (1977).

[2] G. A. Baker and P. R. Graves-Morris, *Padé Approximants*, Cambridge University Press (1996), v. 59.

[3] *Multipoint Padé Approximants* (Wolfram Mathworld).

[4] D. E. Knuth, *The Art of Computer Programming, Seminumerical Algorithms*, 3rd ed., Addison-Wesley Longman Publishing Co., Inc., Boston, MA, USA (1997).

[5] R. E. Ryltsev and N. M. Chtchelkatchev, Phys. Rev. E **88**, 052101 (2013).